Photonic Add-Drop-Gate Node Element Based on EML Technology

Bernhard Schrenk, *Member, IEEE,* and Fotini Karinou, *Member, IEEE*

Abstract—**We propose a novel approach for reconfigurable photonic nodes in short-reach optical networks, which builds on unified component technology for several key functions. The need for fast transmission, reception and switching components is addressed through use of a widely adopted technology that is particularly known for its cost efficiency: the externally modulated laser (EML). Through consequent use of EMLs as fast and versatile electro-optic node element in combination with a slower yet reconfigurable cross-connect matrix serving as interconnection between several elements, a node architecture can be synthesized on demand – such as known from field-programmable gate arrays that have revolutionized the field of programmable microelectronics.**

To prove the proposed multi-functional EML-based approach, we experimentally investigate the capabilities of this photonic transmitter as coherent receiver of dropped signals and as optical gate, being the basic element of fast switches. We first demonstrate the polarization-immune coherent homodyne reception of broadband 10 Gb/s on-off keyed signals without further need for digital signal processing. Transmission is shown at an optical budget of 24 dB and in presence of 12 side-channels. Moreover, the EML is applied as fast 1×1 switch by proving that gating at the sub-ns regime can be facilitated at a reception penalty of less than 1 dB.

Index Terms—**Optical communication terminals, Optical fiber communication, Optical signal detection, Optical switches, Externally modulated laser**

I. Introduction

TRANSCEIVER technology foremost determines the performance of optical links. High energy efficiency, paired with low cost of ownership has enabled the penetration of application domains where photonics has since been a door opener for capacity growth. In the context of networking, transceiver technology and opto-electronics are required to evolve if emerging networking paradigms and a higher degree of flexibility and dynamicity are to be supported. For example, intra-datacenter connectivity strives for optical switching mechanisms at the packet level, featuring a fast sub-ns switching time at low cost. At the same time the migration from direct-detection to coherent reception would unlock further performance gains – as it is also sought for optical access and the mobile fronthaul. There has been a tremendous research effort on both aspects, proposing deployable coherent transceiver technology through the replacement of digital functions by analogue counterparts [1], or greatly simplified coherent transceivers in combination with low-complexity modulation [2]. Besides transceiver sub-systems, switching/gating and filtering functions complement the electro-optical conversion eco-system and promise more efficient network architectures. In this context previous demonstrations include compact tunable ring resonators on silicon [3], arrays of semiconductor optical amplifiers (SOA) or electro-absorption modulators (EAM) as optical gates [4,5], or switches employing novel materials such as lead lanthanum zirconium titanate (PLZT) [6]; however, these works do either lack native optical gain, fast response at the bit level or they do face compatibility issues with well-established integration platforms. Combining all constituent transmission and networking technologies therefore leads to heterogeneous islands of highly specialized components tailored to deliver superior performance for a very specific task in the optical telecommunication landscape. Up to now, no unified platform exists for realizing all the aforementioned key features – transmission, coherent reception and optical switching – in a single platform such as an optical field-programmable gate array (FPGA).

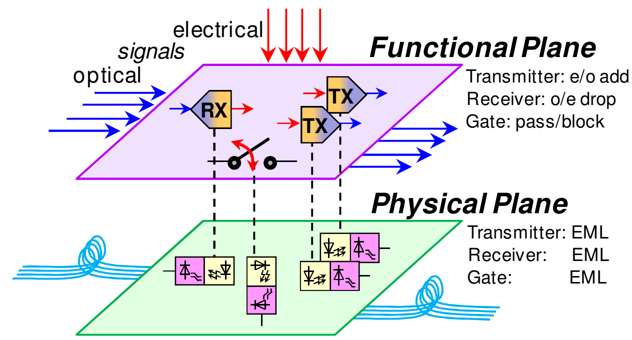

Fig. 1. Multi-functional add-drop-gate node based on EML technology.

In this work, we investigate the feasibility of such a versatile and reconfigurable photonic node for metro-access- and short-reach networks. To do so we experimentally investigate to which extent externally modulated lasers (EML) can accommodate for several of the aforementioned fast

Manuscript received December 13, 2018. This work was partially supported through funding from the European Research Council (ERC) under the European Union's Horizon 2020 research and innovation programme (grant agreement No 804769).

B. Schrenk is with the Austrian Institute of Technology, Center for Digital Safety&Security, Giefinggasse 4, 1210 Vienna, Austria (phone: +43 50550-4131; fax: -4150; e-mail: bernhard.schrenk@ait.ac.at).

F. Karinou is with Microsoft Research Ltd, Cambridge, CB1 2FB, United Kingdom (e-mail: fotini.karinou@microsoft.com).

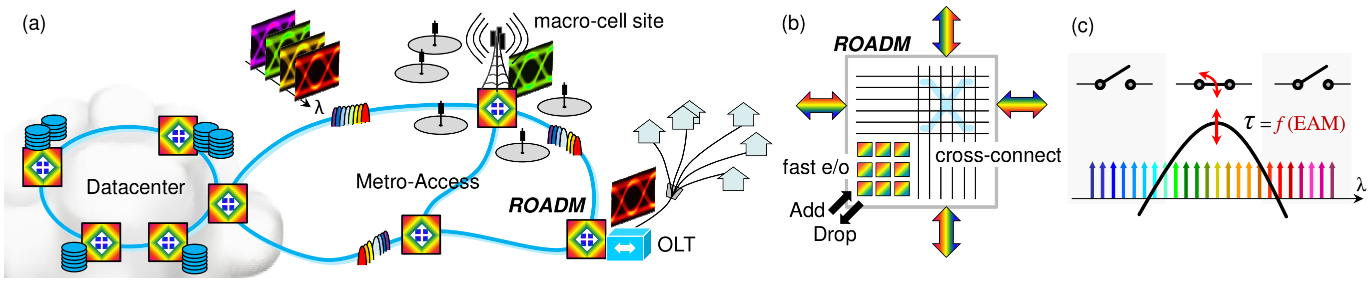

Fig. 2. (a) Metro-access-wireless and datacenter networks backed by photonic nodes reconfigurable in terms of capacity allocation and direction in which bandwidth is provisioned. (b) ROADM following the architecture of a FPGA, featuring fast electro-optical (e/o) functions for signal conversion and switching, which are complemented by a slow cross-connect matrix. (c) EML fiber-to-fiber transmission serving as wavelength-selective optical gate.

electro-optic functions at the physical layer, as sketched in Fig. 1. We demonstrate, for the first time, coherent analogue homodyne reception of 10 GHz broadband signals over a loss budget of 24.4 dB, meaning a 4× bandwidth improvement compared to the previous work [7]. We further evaluate EMLs for optical gating at the bit level with a low penalty of <1 dB.

The paper is organized as follows. Section II sets the scene for reconfigurable photonic nodes in metro-access-wireless and datacenter networks. Section III introduces the EML as key element in such a versatile photonic node and discusses its abilities to realize transmission, reception and gating functions. Section IV elaborates on the experimental evaluation setting that is used for performance evaluation. Section V discusses the results for the EML as coherent drop receiver, while Section VI is dedicated to gating operation. A conclusion is drawn in Section VII and is further complemented by a brief outlook.

II. The Need for Network Node Synthesis

Reconfigurable optical add/drop multiplexers (ROADM) have become indispensable as the "adhesive" in core networks and contribute their unique assets towards the realization of elastic and flexible optical networking [8]. However, the ROADM complexity quickly raises when a multitude of functions such as coherent drop reception and fast switching are to be included. Alternative ROADM solutions that avoid highly specialized components can therefore trade well in terms of cost effectiveness when deployment in shorter-reach networks is considered. Figure 2(a) highlights the use of such simplified photonic nodes with integrated add/drop transponders in access-scale telecom and short-reach datacom networks. With the ongoing wireline-wireless convergence and the introduction of cloud services the metro-access-wireless network experiences a more symmetric and dynamic traffic demand. Sources for dynamicity and symmetry include user mobility between residential, transport and business areas [9], which result in ad-hoc activation and bandwidth provisioning for small radio cells, network-integrated mobile edge computing as exploited in cloud-based radio access networks, or end-user services such as cloud storage or file sharing [10]. Bandwidth in the converged metro-access-wireless network is therefore allocated in a flexible manner in terms of capacity and direction. This can be best supported by employing wavelength division multiplexing with reconfigurable network nodes located at the sites of wireless macro-cells, optical line terminals (OLT) of access networks, or simply along the metro mesh. At the same time, ROADM nodes introduce vital resiliency functionality for the backhaul and feeder infrastructure through network-integrated monitoring and agile switching [11]. Similar demand for flexibility arises within hyperscale datacenters, whose reconfigurable pod networks are trampled by data flows that show a widely varying lifetime. While continuous elephant flows are tolerant to the performance specifications found for circuit switching, the much shorter lived mice flows demand sub-ns switching speed for the photonic nodes found in datacenter networks [12].

Under the umbrella of these two representative network scenarios photonic node technology not only needs to be reconfigurable in terms of networking and add/drop functionality, but shall also accommodate for fast optical switching. A practical approach to support the synthesis of the network infrastructure optimized for a given context and a given traffic demand is the use of a programmable network node. Such architecture-on-demand schemes have been proposed earlier [13] and follow a successful example from the field of microelectronics: the FPGA. By allocating hardware resources such as arithmetic and logic cells towards the required functions while partitioning these cells through a flexible wiring scheme, the optimal node configuration can be synthesized. Figure 2(b) sketches such an FPGA-like approach for the specific case of photonic networks. The FPGA cells relate to opto-electronic conversion functions that contribute towards signal add/drop and fast switching. A slower optical cross-connect matrix shapes the overall ROADM architecture in which the electro-optic cells are being applied. To this end this paper contributes to the question whether low-cost EML-based transceiver technology can fulfill the functions of the cells in such a photonic node.

III. The EML as Versatile Key Element for Optical Nodes with Add-, Drop- and Gating-Functionality

Signal add/drop and switching functions require the conversion from the electrical domain to the optical domain and vice versa, and electro-optical gating. Conceptual simplicity at the physical plane shall be guaranteed by the consequent use of EMLs, which are recognized as well-adopted transmitters in optical telecom and datacom applications. These key elements may be interconnected

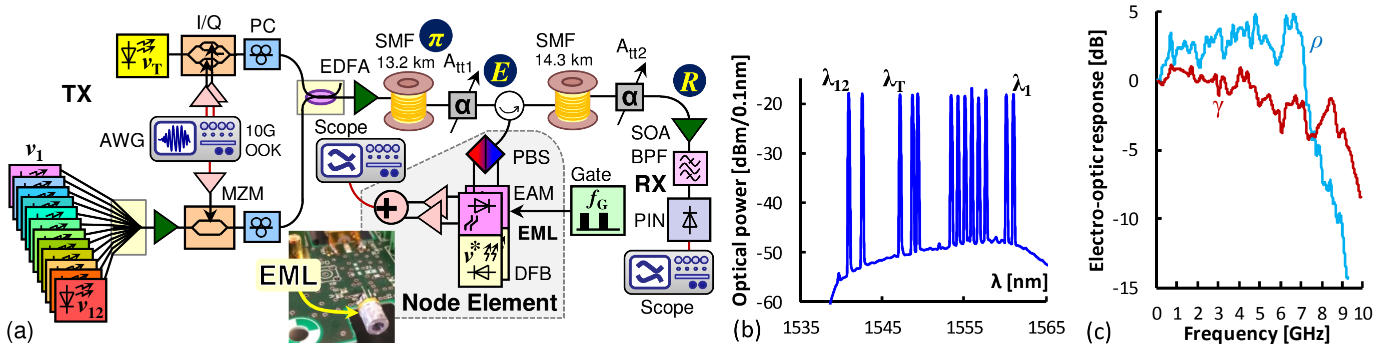

Fig. 3. (a) Experimental setup. (b) Transmitted signal spectrum including the target channel (λ_T) and 12 side-channels ($\lambda_1 \ldots \lambda_{12}$). (c) Electro-optic response for the EML as transmitter (γ) and receiver (ρ).

through simpler, waveguide-based space switches to shape the ROADM in a static or reconfigurable way. Scalable cross-connects based on InP or silicon waveguide technology can be found in previous works, showing non-blocking 8×8 to 32×32 cross-connects [14, 15]. These matrices can be monolithic or hetero-integrated with the EML-based add/drop and gating functions and can serve the wavelength-selective signal filtering by introducing colored switch elements such as ring filters [16, 17]. Therefore this proof-of-concept work is exclusively focusing on the active electro-optic functions enabled through these multi-functional EMLs. The following methodology is applied for the particular ROADM functions.

A. Signal Add: Transmission

EMLs are well understood for optical signal transmission and therefore this aspect is not explicitly repeated in this work. Their large electro-optic bandwidth of more than 100 GHz [18] and their low drive of 65 mV_{pp} per dB of modulation extinction ratio [19] render EMLs as cost- and energy-efficient optical transmitters that are well suited for metro-access and datacenter applications. EML modulation results in double-sideband signals, which is to be taken into consideration for the coherent signal reception intended in this work.

B. Signal Drop: Coherent Reception

In case of drop reception the distributed feedback (DFB) section of the EML serves as local oscillator (LO) λ^* that is aligned to the target channel λ_T by means of injection locking. This yields homodyne reception and thus a 1:1 signal translation between the optical and electrical domain, without additional digital signal processing (DSP) resources and at an increased sensitivity with respect to direct detection. While the principle has been validated earlier in combination with orthogonally frequency division multiplexed passband signals [2], this work demonstrates the first operation for broadband-modulated 10 GHz data signals featuring simple and cost-effective on-off keying. The provision of coherent rather than direct detection without raising the complexity considerably avoids the use of extra reconfigurable WDM components for the purpose of signal selection. Wideband operation for coherent reception but also transmission requires tunable EMLs, which have been demonstrated earlier [20].

C. Fast Gating

In case of gated operation, which corresponds to a 1×1 switch representation, the DFB section of the EML is used as reflective gain element while the EAM is used as blocker. The emission wavelength ν^* of the EML is detuned from the data channels at ν_i so that $B < |\nu^* - \nu_i| < \beta$, where B is the electrical reception bandwidth and β the gain bandwidth determined by the DFB grating of the EMLs. The fiber-to-fiber transmission of the EML can then serve as wavelength-selective optical gate, for which the transmission τ is determined by the loss modulation of the EAM section (Fig. 2(c)). A typical gain bandwidth for the optical gate is ~5 nm, as will be discussed shortly. Together with dense channel packing, as enabled through coherent reception, multiple transmission channels can be addressed. On the other hand, the spectral passband behavior of the EML gate leads to an optical filtering effect, which can be beneficial as it avoids additional WDM filters. Wideband gating and signal selection is again bound towards tunable EML technology, while the composition of 1×N switch configurations is thinkable through an interconnection of optical gates.

It shall be noted that the aforementioned functions can be realized through use of EMLs, without requiring specific modifications on the optical layer in order to implement each of the functions. For example, the EML can serve as either transmitter or receiver through a simple change of RF front-end functions in the electrical domain, which corresponds to the substitution of a driver with a low-noise amplifier or vice versa. By applying a hardware-independent approach, the chosen photonic technology fits squarely to a reconfigurable node architecture that can be modified on demand. On top of this, simultaneous operation of the EML as transmitter and coherent receiver has been demonstrated recently in combination with electrical passband signals [21] and promises and even higher degree of flexibility.

IV. Evaluation Methodology and Experimental Setup

The proposed node elements for drop and gate functions have been experimentally evaluated. The setup is presented in Fig. 3(a). The versatile EML-based node element connects a remote transmitter with a receiver through two spans of 13.2 and 14.3 km of single-mode fiber (SMF). This emulates a scenario where the node is situated in the middle of a communication link. At the remote transmitter a target channel

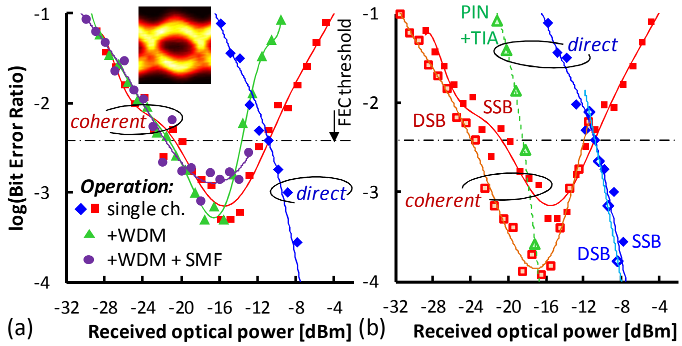

Fig. 4. (a) BER performance for coherent / direct detection with EML-based drop receiver for SSB data and (b) comparison with DSB.

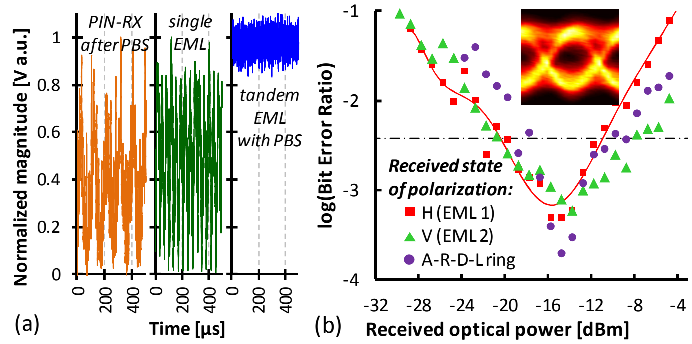

Fig. 5. (a) Polarization immune EML receiver and (b) BER performance.

at λ_T = 1547.2 nm is modulated with 10 Gb/s on-off keyed data and launched together with 12 modulated side-channels (λ_1...λ_{12}) in the C-band (Fig. 3(b)) at a power level of 3 dBm/λ. In case of drop reception at the node, the LO (λ*) of the transistor-outline (TO) packaged EML is locked to the target channel λ_T by means of current and temperature tuning so that injection locking occurs when the wavelengths λ_T and λ* fall within the locking range [2]. The electro-optic bandwidth of the employed EMLs is presented in Fig. 2(c) for an EML used as receiver (ρ) and as transmitter (γ). The latter applies to the operation mode as a fast optical gate. When the rather pronounced ripple in the response is ignored, the bandwidth is 7.2 and 7.3 GHz, respectively.

In view of coherent reception with a possible frequency detuning between LO and incident data signal an I/Q modulator was used at the remote transmitter. In this way single- (SSB) and double-sideband (DSB) modulated data signals can be both evaluated. Polarization immunity for the homodyne receiver is provided through a diversity scheme using a tandem of EMLs in combination with a polarization beam splitter (PBS), as it was previously introduced [7]. Error counting for the dropped signal is performed after acquisition through a real-time oscilloscope.

Optical gating at the node can be supported by leaving the LO of the EMLs detuned and yet in the spectral vicinity of the selected data channels. In case of blocking operation at the optical gate, a gating signal with a repetition rate of f_G = 9.84 MHz blanks the data after four pseudo-random bit sequences (PRBS) of length 2^7-1 through signal extinction by optical loss modulation with the EML. The choice in favor of this short PRBS length was made to emulate short-lived mice flows [12] and for the sake of pattern traceability in the acquired signal. The chosen timing corresponds to a short packet length of 50.8 ns and a duty cycle of 50% for the data frame. In case of pass-through operation, meaning a transparent gate state, the signals are forwarded to a SOA+PIN based receiver after selecting the target channel λ_T by means of optical bandpass filtering (BPF). Variable attenuators (A_{tt1}, A_{tt2}) have been used to set the delivered optical power to the optical gate and for the purpose of BER measurements.

V. Coherent Homodyne Drop Functionality through an EML as Broadband Receiver

The BER performance for 10 Gb/s SSB on-off keyed signal reception with a single EML is shown in Fig. 4(a). The incident polarization state has firstly been manually aligned to yield optimal response for signal reception. Back-to-back measurements are presented for single-channel transmission and coherent detection (■) in comparison with direct detection (◆) using the same EAM photodiode.

The correct operation of the coherent homodyne reception scheme is evidenced by the clear eye opening, which confirms that there is no frequency detuning between LO and incident data signal. The reception performance has been referenced to a forward error correction (FEC) level as these codes are typically considered for short-reach and access applications. A reception sensitivity of -20.9 dBm at the hard-decision FEC level of 3.8×10^{-3} is obtained for coherent reception (■) even though no transimpedance amplifier (TIA) was used after the EAM due to packaging restrictions arising from the TO-can outline of the EML. Further improvement is therefore expected once the 50Ω pre-amplifier used in this work is replaced by a TIA. At the same time a closer co-integration of EAM detector and electrical front-end is expected to eliminate the strong ripple in the electro-optic response, which together with the current EAM bandwidth is seen as a limitation for the current reception performance. Overload can be noticed at higher input power levels, for which the BER surpasses the FEC threshold due to distortion arising from direct-detection terms. However, when deactivating the LO so that the EML performs direct detection (◆), an input power level of 0 dBm is still permissible although the sensitivity of the direct-detection receiver greatly drops to -10.8 dBm at the FEC level. By exploiting both, coherent and direct detection regimes, the dynamic range can be doubled to more than 21 dB.

The EML function as filtered coherent receiver and the stability of the injection locking process have been evaluated through transmission of 12 modulated DWDM side-channels. All side-channels have been injected to the C-band EML to investigate a possible performance degradation due to cross-talk or overload. There was no penalty in sensitivity (▲) and the locking of the LO remained stable. However, overloading occurs earlier. When adding the transmission fiber a similar performance can be obtained (●). An optical loss budget of

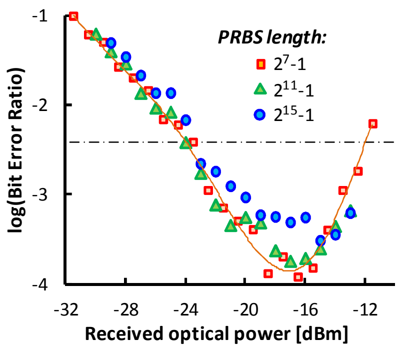

Fig. 6. BER performance as function of the PRBS length for coherent reception of DSB signals with a single-polarization EML receiver.

24.4 dB can be supported for the given launch of 3 dBm/λ at the transmitter.

While coherent detection often requires digital signal recovery, this work features a simpler and more cost-effective reception scheme that solely relies on analogue components. However, applying SSB modulation at the transmitter offsets this cost reduction obtained at the drop receiver of the node. Therefore reception of DSB signals has been also investigated. Figure 4(b) presents a comparison between the coherent (■,□) and direct (◆,◇) reception of 10 Gb/s SSB (■,◆) and DSB (□,◇) data signals. The correct frequency translation of the homodyne reception scheme not only enables DSP-less SSB but also DSB reception. Even for fiber transmission the DSB signal experiences a slightly better sensitivity. This is explained by the penalty inherent to the method that is applied for generating the SSB signal [22], which additionally requires a careful adjustment of the I/Q bias points at the transmitter.

Figure 4(b) also shows a comparison with a PIN/TIA (△) replacing the EML when receiving a 10 Gb/s DSB signal. As it is expected, the TIA front-end performs better than the direct-detection EAM receiver with 50Ω low-noise amplifier. The notable difference in reception sensitivity (△,□) gives an indication that the coherent reception performance can be further increased through co-integration of the EML with a TIA.

Polarization immunity for coherent drop reception is facilitated through a tandem of EMLs in a polarization diversity arrangement. The SMF at point π in the experimental setup (Fig. 3(a)) was temporarily replaced by a polarization scrambler for characterization purposes and a radio frequency (RF) tone was transmitted as probe signal. Figure 5(a) presents the received relative magnitude of this tone for detection with (i) a PIN photodetector after a fiber-PBS, (ii) a single-ended EML without polarization optics and (iii) the combined signal of a tandem EML at both branches of a fiber-PBS. The scrambling of the incident polarization state leads to strong amplitude fluctuations, while for the diversity receiver a steady amplitude is obtained.

The resulting BER performance for the diversity receiver is shown in Fig. 5(b). When the polarization state is manually optimized for either of the two reception bases (H,V), a similar BER performance can be obtained for the two EML branches (■,▲). When injecting a worst-case polarization state

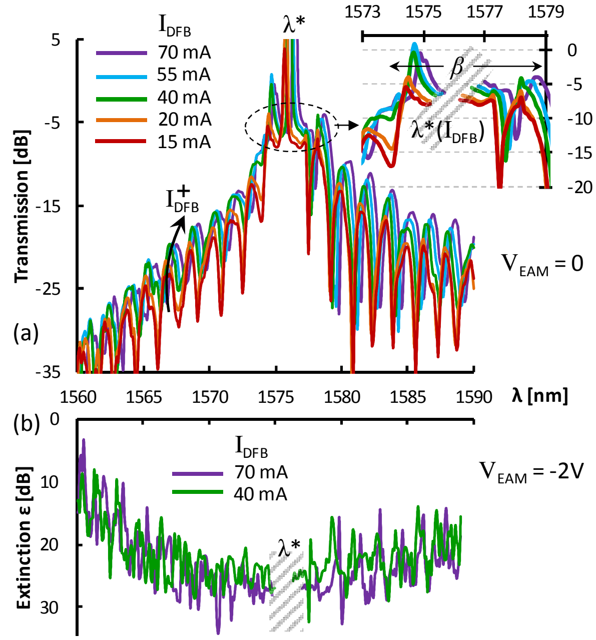

Fig. 7. Fiber-to-fiber transmission and extinction ε of an EML-based gate. Measurements are shown for an L-band EML device with integrated coupling optics, substituting the C-band EML of the experiment to yield an optimized fiber-to-fiber response for characterization purposes.

for which the Stokes vector would be positioned on the meridian of the Poincaré sphere that spans through circular and diagonal states, the sensitivity decreases by 1.9 dB, which is an acceptable trade-off for obtaining polarization-immune operation. It shall be noted that for the diversity receiver each EML branch is independently locked to the incident signal [7].

Coherent homodyne reception exploiting injection locking requires to investigate the robustness of the proposed EML-based receiver for a longer number of consecutive identical bits in the received data stream. The BER performance for different PRBS lengths has been therefore analyzed for a single-polarization EML receiver and DSB modulation for the data signal. Results are presented in Fig. 6. Although a PRBS with 2^{15}-1 length (●) leads to a BER increase with respect to a short 2^7-1 PRBS (■) in optimal received power level range from -14 to -20 dBm, the BER remains well below the FEC threshold so that the dynamic range at the FEC level is not notably restricted.

VI. Fast Blocking at the Packet Level through an EML as a Reflective Optical Gate

When the EML is exploited as an optical gate, the incident data signal is brought to the DFB gain region in the vicinity of the emission wavelength λ* rather than being aligned to it as for the case of coherent homodyne detection. Figure 7(a) shows the reflective fiber-to-fiber transmission of an EML. Characterization data is shown for an L-band TO-can EML with integrated lens since the fiber coupling optics for the C-band EML used for the actual transmission experiments were sub-optimal, hence leading to excess coupling loss. The emission wavelength λ* of this EML was 1576.5 nm for a bias current of 70 mA. For the pass-through state (V_{EAM} = 0) the

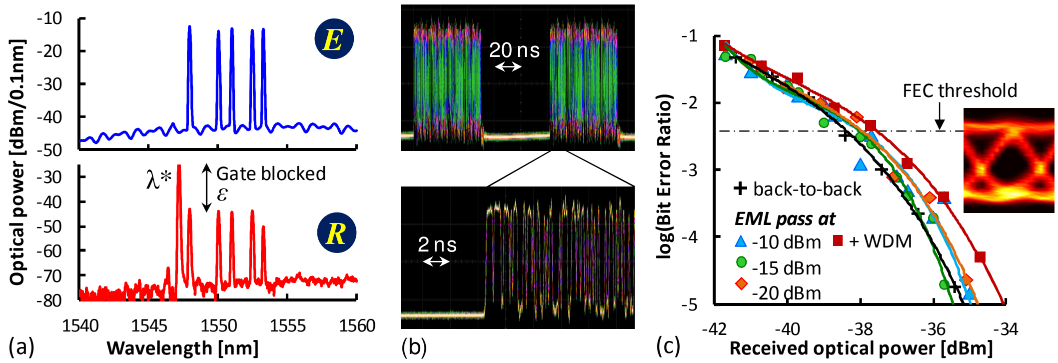

Fig. 8. (a) Static spectrum at the input of the EML gate and the receiver at the output of the gate. (b) Trace of gated signal and (c) BER performance.

transmission of the L-band EML is 0 to -6 dB for the spectral region λ* +2.7/ 2.9 nm (β = 5.6 nm) at a DFB bias of I_{DFB} = 70 mA. This transmission value results from the bidirectional fiber-to-chip coupling, the EAM pass-through loss and the gain contributed by the DFB section. Figure 7(b) presents the gate extinction ε for an EAM bias of V_{EAM} = -2V. The extinction is better than 23.7 dB at the DFB gain region, meaning a good signal suppression during the blocking state of the optical gate.

The spectral roll-off of the DFB gain leads to suppression of wavelengths remote from the nominal EML emission wavelength λ*, while channels in its vicinity can be passed through the gate by EAM bias adjustment. In this way the EML operates as wavelength-selective gate. Figure 8(a) shows the static spectrum for gating 5 input signals with the original C-band EML. The channels are suppressed by the extinction ε. The outermost channel at 1553.3 nm is already located at the roll-off of the DFB.

Fast gating can be performed in virtue of the EAM's large electro-optical bandwidth. Figure 8(b) shows the 10 Gb/s data signal launched at 1550.1 nm and received by the filtered SOA+PIN receiver after passing through the EML-based node element, which serves as optical gate. The periodic gating signal described in Section IV leads to the intended optical carving of four PRBS sequences per packet with steep and clear packet edges. The rise/fall time is less than 100 ps, which makes the EML suitable for precise gating of short-lived mice flows.

The BER performance for gated operation is discussed in Fig. 8(c). The 10 Gb/s back-to-back sensitivity of the SOA+PIN receiver was -38.4 dBm at the FEC threshold (+). Packet-level BER results are shown for single-channel fiber transmission and an injection level of -10 (▲), -15 (●) and -20 dBm (◆) at the input of the EML gate. The reception penalty is 0.4 dB at the FEC threshold. It is insensitive to the injection level given the high OSNR value of 27 dB for the lowest feed power. The compatible per-span loss budget is 17.5 dB before and after the EML-based optical gate. A low extra penalty of 0.5 dB confirms the correct gate operation in presence of 4 modulated DWDM side-channels (■) at an injection level of -10 dBm/λ.

The re-utilization of optical spectrum originally occupied by signals that are dropped by the optical gate requires an analysis of the crosstalk that is induced due to a finite gate extinction. For this purpose a signal has been added after the optical gate. Figure 9(a) shows the experimental setup that investigates this case. A 10 Gb/s DSB data signal that is to be dropped is transmitted by a Mach-Zehnder modulator (MZM) at $\lambda_{T,Drop}$ and fed to the optical gate composed by a single-polarization EML. The output of the gate is combined with an added signal using a colorless 50/50 coupler. In this way either the signal passed by the gate or the added signal are forwarded by the node and further acquired by the SOA+PIN receiver.

The added 10 Gb/s signal is launched at 3 dBm by a second EML emitting at $\lambda_{T,Add}$ = $\lambda_{T,Drop}$ and therefore in spectral overlap the wavelength of the drop signal. A high suppression of the drop channel is paramount to avoid crosstalk from the dropped to the added channel. The received optical signal spectra are presented in Fig. 9(b) for the dropped signal when passed (□) and rejected (◇) by the optical gate without subsequent "add" operation, and for adding a channel when the optical gate passes (■) and rejects (◆) the drop signal. The power difference of 10.6 dB between the launch of the added channel and the delivered power level of the dropped signal to the node adds on top of the gate rejection. Figure 9(b) also shows the DFB emission wavelength λ*, which is on the upper side in this case.

The penalty in reception sensitivity due to a signal that is added on a dropped channel can be seen in Fig. 9(c). BER measurements have been conducted in continuous mode, meaning a temporal overlap of the dropped and added signal at any time. The penalty for the added channel without crosstalk-inducing drop signal at the input of the optical gate (▲) is less than 1 dB at a BER of 10^{-5} with respect to the back-to-back performance of the SOA+PIN receiver (+). This small penalty is attributed to the imperfection of the EML transmitter in terms of electro-optic modulation bandwidth compared to the ideal MZM that has been used for the back-to-back measurements.

Severe crosstalk makes signal transmission for the added signal impossible when an optical drop signal at the input of the gate is passed. This is evidenced by the eye of the added signal for this present state of the drop signal without rejection. When the optical gate is opened, meaning that the drop signal is present at the gate input yet rejected (◆), a nearly identical BER performance can be obtained as for a

This is the author's version of an article that has been published in this journal. Changes were made to this version by the publisher prior to publication.
The final version of record is available at http://dx.doi.org/10.1109/JLT.2019.2906075

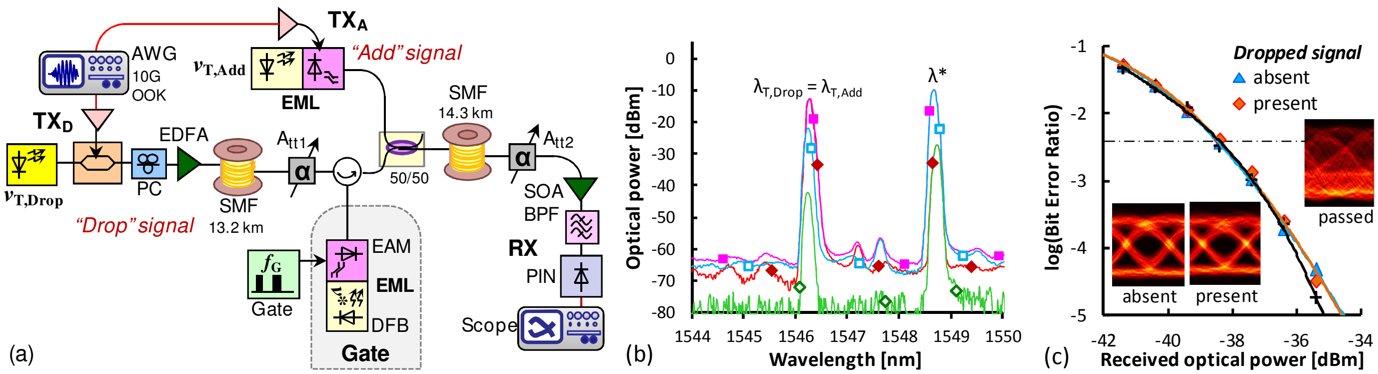

Fig. 9. (a) Experimental setup for adding a spectral add channel onto a dropped signal. (b) Received signal spectra for various conditions of adding a channel and rejecting the drop signal incident to the gate. (c) BER performance for the added channel under an open gate for which the dropped signal is present but rejected, and for an absent drop signal at the optical gate input.

drop signal that is absent at the gate input (▲). This confirms the good crosstalk suppression through the EML-based optical gate in addition to the natural power difference between the add channel and the received drop channel.

VII. Conclusion

EML technology has been evaluated as coherent drop receiver and fast optical gate element. DSP-less coherent homodyne reception of 10 Gb/s on-off keyed signals is compatible with optical budgets of 24.4 dB even though no TIA has been used as electrical amplifier. Diversity reception with a tandem EML reduces the worst-case polarization penalty to 1.9 dB. Moreover, operation with double-sideband modulation and 12 DWDM side-channels has been validated. Fast optical blocking with a penalty of <1 dB proved feasible in the vicinity of 5.6 nm around the EML emission wavelength. The rejection of the optical gate is high enough to allow for re-use of spectral channels in a drop-before-add architecture.

The flexibility of an EML to serve as multi-functional element and the provided experimental results open vistas towards the formation of photonic node technology, following the architecture-on-demand paradigm. To do so, sub-system level improvements such as TIA co-integration for enhanced reception performance and integration of fast EML components in a slower yet reconfigurable cross-connect matrix are required.

References

[1] M. Morsy-Osman et al., "DSP-free 'coherent-lite' transceiver for next generation single wavelength optical intra-datacenter interconnects," *OSA Opt. Expr.*, vol. 26, no. 7, pp. 8890-8903, 2018.
[2] B. Schrenk, "Injection-Locked Coherent Reception Through Externally Modulated Laser," *IEEE J. Sel. Topics in Quantum Electron.*, vol. 24, no. 2, p. 3900207, Mar. 2018.
[3] Z. Guo, L. Lu, L. Zhou, L. Shen, and J. Chen, "16 × 16 Silicon Optical Switch Based on Dual-Ring-Assisted Mach–Zehnder Interferometers," *IEEE/OSA J. Lightwave Technol.*, vol. 36, no. 2, pp. 225-232, Jan. 2018.
[4] R. Stabile, A. Rohit, and K.A. Williams, "Monolithically Integrated 8×8 Space and Wavelength Selective Cross-Connect," *IEEE/OSA J. Lightwave Technol.*, vol. 32, no. 2, pp. 201-207, Jan. 2014.
[5] Y. Muranka et al., "Monolithically Integrated 4×4 Optical Switch with Cascaded MZIs and EAM-Gate Array," in *Proc. Europ. Conf. Opt. Comm. (ECOC)*, Dusseldorf, Germany, Sep. 2017, P1.SC2.33.
[6] G. Hu, Z. Qi, B. Yun, R. Zhang, and Y. Cui, "Compact, integrated PLZT optical switch array," *OSA Chin. Opt. Lett.*, vol. 13, no. 11, p. 111301, 2015.
[7] B. Schrenk, and F. Karinou, "Polarization-Immune Coherent Homodyne Receiver Enabled by a Tandem of TO-can EMLs," in *Proc. Europ. Conf. Opt. Comm. (ECOC)*, Rome, Italy, Sep. 2018, We4G.3.
[8] S. Gingeri et al., "Flexible Architectures for Optical Transport Nodes and Networks," *IEEE Comm. Mag.*, vol. 48, pp. 40-50, Jul. 2010.
[9] H. Wang, F. Xu, Y. Li, P. Zhang, and D. Jin, "Understanding Mobile Traffic Patterns of Large Scale Cellular Towers in Urban Environment," in *Proc. ACM IMC 2015*, Tokyo, Japan, Oct. 2015, S6.1.
[10] Z. Aouini, A. Kortebi, and Y. Ghamri-Doudane, "Towards understanding residential internet traffic: From packets to services," in *Proc. Int. Conf. on the Netw. of the Future (NOF)*, Buzios, Brazil, Nov. 2016, pp. 1-7.
[11] B. Schrenk, F. Laudenbach, R. Lieger, T. Lorünser, P. Bakopoulos, A. Poppe, M. Stierle, H. Avramopoulos, and H. Leopold, "Passive ROADM Flexibility in Optical Access with Spectral and Spatial Reconfigurability," *IEEE J. Sel. Areas of Comm.*, vol. 33, no. 12, pp. 2837-2846, Sept. 2015.
[12] T. Benson, A. Akella, and D. Maltz, "Network Traffic Characteristics of Data Centers in the Wild," in *Proc. ACM SIGCOMM Conf. Internet Meas.*, Melbourne, Australia, Nov. 2010, pp. 267-280.
[13] M. Garrich et al., "Experimental Demonstration of Function Programmable Add/Drop Architecture for ROADMs," *IEEE/OSA J. Opt. Comm. Netw.*, vol. 7, no. 2, pp. A1-A9, Feb. 2015.
[14] M.J. Kwack, T. Tanemura, A. Higo, and Y. Nakano, "Monolithic InP strictly non-blocking 8x8 switch for high-speed WDM optical interconnection," *OSA Opt. Expr.*, vol. 20, no. 27, pp. 28734-28741, Dec. 2012.
[15] L. Qiao, W. Tang, and T. Chu, "32 × 32 silicon electro-optic switch with built-in monitors and balanced-status units," *Sci. Rep.*, vol. 7, p. 42306, Feb. 2017.
[16] F. Xu, and A.W. Poon, "Silicon cross-connect filters using microring resonator coupled multimode-interference-based waveguide crossings," *OSA Opt. Expr.*, vol. 16, no. 12, pp. 8649-8657, Jun. 2008.
[17] Y. Goebuchi, M. Hisada, T. Kato, and Y. Kokubun, "Optical cross-connect circuit using hitless wavelength selective switch," *OSA Opt. Expr.*, vol. 16, no. 2, pp. 535-548, Jan. 2008.
[18] O. Ozolins et al., "100 GHz EML for High Speed Optical Interconnect Applications," in *Proc. Europ. Conf. Opt. Comm. (ECOC)*, Düsseldorf, Germany, Sep. 2016, M2C4.
[19] H. Dalir, Y. Takahashi, F. Koyama, "Compact low driving voltage (<400 mV$_{pp}$) electro-absorption modulator laterally integrated with VCSEL," *Electron. Lett.*, Vol. 50, no. 2, pp. 101- 103, Jan. 2014.
[20] T. Tanbun-Ek et al., "Broad-Band Tunable Electroabsorption Modulated Laser for WDM Application," *IEEE J. Sel. Topics in Quantum Electron.*, vol. 3, no. 3, pp. 960-967, Jun. 1997.
[21] B. Schrenk, and F. Karinou, "World's First TO-can Coherent Transceiver," in *Proc. Opt. Fiber. Comm. Conf. (OFC)*, San Diego, United States, Mar. 2018, Th1A.4.
[22] D. Fonseca, A.V.T. Cartaxo, and P. Monteiro, "Optical Single-Sideband Transmitter for Various Electrical Signaling Formats," *IEEE/OSA J. Lightwave Technol.*, vol. 24, no. 5, pp. 2059-2069, May 2006.

Bernhard Schrenk (S'10-M'11) was born 1982 in Austria and received the M.Sc. ('07) degree in microelectronics from the Technical University of Vienna. He was at the Institute of Experimental Physics of Prof. A. Zeilinger, where he was involved in the realization of a first commercial prototype for a quantum cryptography system, within the European SECOQC project. From 2007 to early 2011 he obtained his Ph.D degree at UPC BarcelonaTech, Spain. His Ph.D thesis on multi-functional optical network units for next-generation Fiber-to-the-Home access networks was carried out within the FP7 SARDANA and EURO-FOS projects. In 2011 he joined the Photonic Communications Research Laboratory at NTUA, Athens, as post-doctoral researcher and established his research activities on coherent FTTH under the umbrella of the FP7 GALACTICO project. In 2013 he established his own research force on photonic communications at AIT Austrian Institute of Technology, Vienna, where he is working towards next-generation metro-access-5G networks, photonics integration technologies and quantum optics.

Dr. Schrenk has authored and co-authored ~125 publications in top-of-the-line (IEEE, OSA) journals and presentations in the most prestigious and highly competitive optical fiber technology conferences. He was further awarded with the Photonics21 Student Innovation Award and the Euro-Fos Student Research Award for his PhD thesis, honoring not only his R&D work but also its relevance for the photonics industry. He was elected as Board-of-Stakeholder member of the Photonics21 European Technology Platform in 2017. During his extensive research activities he was and is still engaged in several European projects such as SARDANA, BONE, BOOM, APACHE, GALACTICO, EURO-FOS and the Quantum Flagship project UNIQORN. In 2013 he received the European Marie-Curie Integration Grant WARP-5. In 2018 he was awarded by the European Research Council with the ERC Starting Grant COYOTE, which envisions coherent optics everywhere.

Fotini Karinou was born in Arta, Greece, in 1983. She received the Diploma in Electrical and Computer Engineering, with specialization in telecommunications and information theory, and the PhD degree in optical communications focused on spectrally efficient WDM optical interconnect networks with advanced modulation formats, from the University of Patras, Greece, in 2007, and 2012, respectively. In 2007, she was a visiting researcher in the Institute for Quantum Optics and Quantum Information (IQOQI), at Vienna University of Technology, participating in the initial attempts for the realization of a commercial prototype of a quantum key distribution (QKD) system based on polarization entanglement in the Institute of Experimental Physics of Prof. Zeilinger. In 2011 to 2012, she was a visiting researcher at Denmark Technical University, Photonics Department, where she worked toward spectrum-flexible cognitive optical networks, hybrid optical fiber-wireless transmission and advanced modulation techniques for high-performance computing optical interconnects. From February 2013 to June 2018, Dr. Karinou worked as a Senior R&D Engineer in the Optical Technology Department, later restructured to Optical & Quantum Laboratory, at Huawei Technologies Duesseldorf GmbH, in the German Research Center in Munich, toward next generation high-capacity coherent systems for long reach, high data-rate metro/access optical networks, optical interconnects for data centers and quantum communications. In July 2018 she joined the Systems and Networking Group at Microsoft Research Ltd in Cambridge, UK. She has authored and co-authored more than 65 publications in the highest prestigious optical communications technology journals and conferences. Dr. Karinou has been engaged in several European research projects such as EU FP6 SECOQC, EU FP7 ICT-BONE, EU FP7 CHRON, and H2020 ROAM projects.